

## Melting Behavior of Noble-Metal-Based Bimetallic Clusters\*

Tsung-Wen Yen, P. J. Hsu, and S. K. Lai<sup>†</sup>

*Complex Liquids Laboratory, Department of Physics,  
National Central University, Chungli 320 Taiwan*

(Received 2 November 2008; Accepted 24 January 2009; Published 7 March 2009)

The isothermal Brownian-type molecular dynamics simulation was applied to study the melting scenario of noble-metal-based bimetallic clusters. The failure of the simulation results to portend a compatible melting temperature,  $T_{\text{melt}}$ , which is defined in the specific heat  $C_V$  at its principal peak and in the Lindermann-like parameter at the temperature which it exhibits drastic change, has prompted us to calculate the velocity autocorrelation function VACF or its Fourier-transform, the power spectrum as another useful variable for describing cluster melting. Two bimetallic clusters, namely  $\text{Ag}_{13}\text{Au}_1$  and  $\text{Ag}_{13}\text{Cu}_1$ , were selected for illustration. We effected comparative studies of the thermal and dynamic properties of the  $\text{Ag}_{13}\text{Au}_1$ ,  $\text{Ag}_{13}\text{Cu}_1$  and  $\text{Ag}_{14}$  and explored isothermally the VACF and spectral density of individual atoms in each of these clusters as well as the corresponding whole cluster. We examined, in particular, the influence of the impurity atoms Au and Cu. It is observed that the  $C_V$  of  $\text{Ag}_{14}$  displays a prepeak which is absent in  $\text{Ag}_{13}\text{Au}_1$  and  $\text{Ag}_{13}\text{Cu}_1$ . The physical origin of this prepeak feature was studied and its presence is ascribed to the migrational relocation of the adatom in the cluster. From the temperature change of VACF and spectral density, we deduced  $T_{\text{melt}}$ . It is found that the calculated  $T_{\text{melt}}$  inferred from VACF and power spectrum agrees quite well with that determined from the main peak position of  $C_V$ .

[DOI: 10.1380/ejssnt.2009.149]

Keywords: Molecular dynamics; Clusters; Surface melting

### I. INTRODUCTION

A bulk system in a solid phase would transform to a liquid phase if enough heat is transmitted into it until it attains a specific temperature, say  $T_{\text{melt}}$ . If one were to examine its specific heat  $C_V(T)$  as a function of temperature, either experimentally or theoretically, one will find that  $C_V$  exhibits a sharp peak at  $T_{\text{melt}}$ , manifesting a thermodynamic first-order phase transition. If, in addition, one proceeds to calculate the relative root-mean-square bond length fluctuation parameter  $\delta(T)$  (Lindermann parameter), one will find also that  $\delta$  increases abruptly at or very close to  $T_{\text{melt}}$ . Thus the temperature  $T_{\text{melt}}$  at which both  $C_V$  and  $\delta$  undergo drastic changes is commonly defined in the literature as the melting temperature of a bulk system. These congruous characteristic features of  $C_V$  and  $\delta$  at  $T_{\text{melt}}$  are no longer observed for a finite system such as a cluster [1–3]. In our recent works [2, 3], we have in fact learnt that  $\delta$  is not a useful parameter for espying  $T_{\text{melt}}$  since it increases anomalously at a temperature much lower than  $T_{\text{melt}}$  and may even show rising behavior in multi-steps [2–8]. The cause for this anomalous behavior is now understood to originate with the permutational isomer transition or, in such case as the 14-atom cluster, the migrational relocation of adatom. In view of these studies, it would appear that there is still a need to seek for another ‘phase-transition’ variable. In this work, we draw attention to the velocity autocorrelation function (VACF) and its Fourier-transformed function, the power spectrum. These dynamical quantities were recently examined [3] to exhibit thermal variations

that may be analyzed to pinpoint a  $T_{\text{melt}}$  which is compatible with that deduced from  $C_V$ . As concrete illustrations, we extend our investigation of noble-metal-based bimetal-

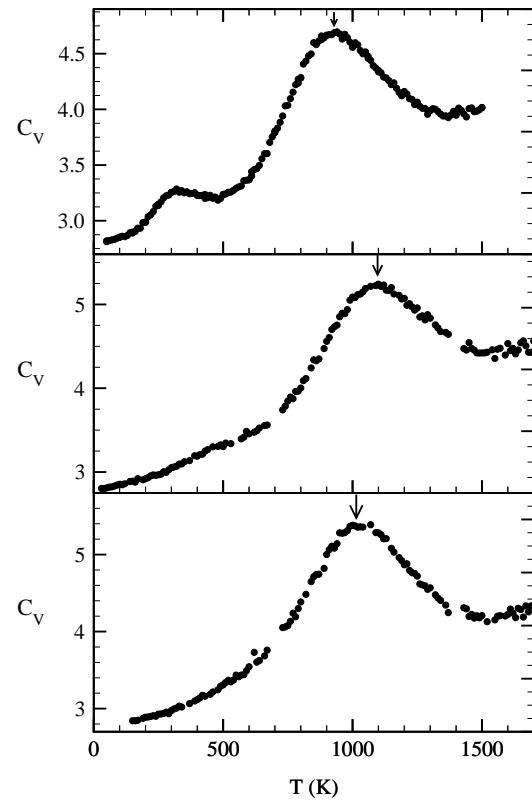


FIG. 1: The constant volume specific heat  $C_V$  for  $\text{Ag}_{14}$  (top),  $\text{Ag}_{13}\text{Au}_1$  (middle) and  $\text{Ag}_{13}\text{Cu}_1$  (bottom). In each case the melting temperature  $T_{\text{melt}}$  is indicated by an arrow and the simulation runs were carried out at  $\Delta t = 5 \times 10^{-15}$  s for  $\text{Ag}_{14}$ ,  $10^{-15}$  s for  $\text{Ag}_{13}\text{Au}_1$  and  $5 \times 10^{-15}$  s for  $\text{Ag}_{13}\text{Cu}_1$ .

\* This paper was presented at International Symposium on Surface Science and Nanotechnology (ISSS-5), Waseda University, Japan, 9–13 November, 2008.

<sup>†</sup>Corresponding author: [sklai@coll.phy.ncu.edu.tw](mailto:sklai@coll.phy.ncu.edu.tw)

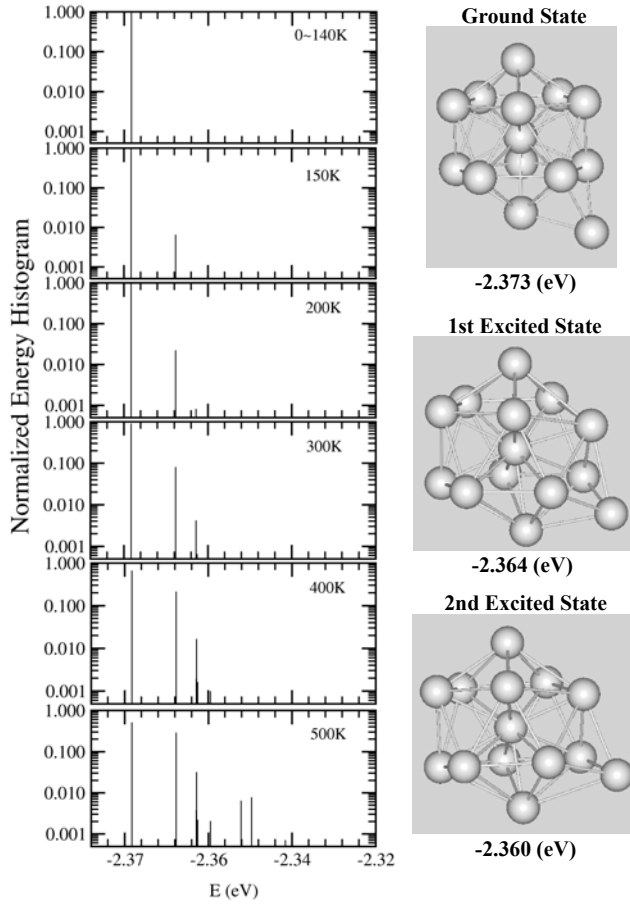


FIG. 2: Energy histograms and structures of the lowest, first and second excited states for metallic cluster  $\text{Ag}_{14}$ . Energy histograms were constructed from isothermal Brownian-type MD simulations at temperatures  $T = 0 \sim 140, 150, 200, 300, 400$  and  $500$  K which cover the prepeak of  $C_V$ .

lic clusters further to  $\text{Ag}_{13}\text{M}_1$  ( $\text{M}=\text{Au}$  and  $\text{Cu}$ ) using the same Brownian-type molecular dynamics (MD) technique as we previously [3] applied to copper-based clusters.

## II. THEORY

### A. Simulation Method

The isothermal Brownian-type MD has been previously introduced and we refer the interested readers to Refs. [1–3] for technical details and for formulas used in the simulation. To implement the MD algorithm, the many-body potential which accounts for the interactions between atoms is indispensable. Here we employ as in our previous works [1–3] the empirical  $n$ -body Gupta potential which is given by

$$E_n = \sum_{i=1}^n \left\{ \sum_{j=1(j \neq i)}^n A_{ij} \exp \left[ -p_{ij} \left( \frac{r_{ij}}{r_{ij}^{(0)}} - 1 \right) \right] - \left[ \sum_{j=1(j \neq i)}^n \xi_{ij}^2 \exp \left( -2q_{ij} \left( \frac{r_{ij}}{r_{ij}^{(0)}} - 1 \right) \right) \right]^{1/2} \right\}. \quad (1)$$

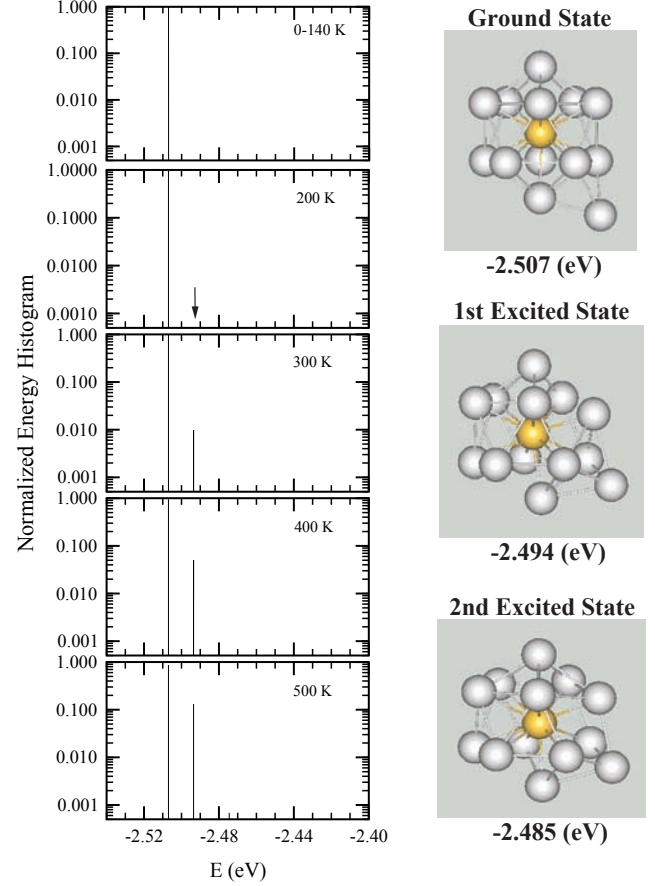


FIG. 3: Same as Fig. 2 but for  $\text{Ag}_{13}\text{Au}_1$ . The arrow at  $T = 200$  K is the first excited state but on the scale of this figure is vanishingly small.

The parameters  $A_{ij}$ ,  $p_{ij}$ ,  $q_{ij}$ ,  $\xi_{ij}$  and  $r_{ij}^{(0)}$  for the Ag and Ag-Au are taken from Rapallo, et al. [9] and their numerical values are given in Table I. For the Ag-Cu, we refer to our previous article [3] and the work of Mottet, et al. [10] to which we consulted.

### B. Thermal and Dynamical quantities

For the thermal and dynamical properties of interest in this work, we calculate the specific heat at constant volume  $C_V$  and the velocity autocorrelation function  $C^{(i)}$  for  $i$ th atom in the cluster; these quantities are given by the following equations.

(a) Specific heat:

$$C_V = \frac{\langle E_{\text{total}}^2 \rangle_t - \langle E_{\text{total}} \rangle_t^2}{k_B T^2} \quad (2)$$

(b) The  $i$ th atom velocity autocorrelation function and power spectrum:

$$C^{(i)}(t) = \frac{\sum_{j=1}^M \vec{v}_i(t_{0j}) \cdot \vec{v}_i(t_{0j} + t)}{\sum_{j=1}^M \vec{v}_i(t_{0j}) \cdot \vec{v}_i(t_{0j})}, \quad (3)$$

$$\Omega^{(i)}(\omega) = 2 \int_0^\infty dt C^{(i)}(t) \cos \omega t. \quad (4)$$

TABLE I: Gupta-type potential parameters for the bimetallic clusters Ag-Au taken from Rapallo et al. [9]. The  $r_{ij}^{(0)}$  for Ag-Au is calculated by averaging the  $r_{ij}^{(0)}$  of Ag-Ag and Au-Au and is scaled by the Bohr radius.

$ij$	$A_{ij}$ (eV)	$\xi_{ij}$	$p_{ij}$	$q_{ij} @$	$r_{ij}^{(0)}$
Au-Au	0.2096	1.8153	10.139	4.033	2.885
Ag-Au	0.1490	1.4874	10.494	3.607	2.8875
Ag-Ag	0.1031	1.1895	10.850	3.180	2.89

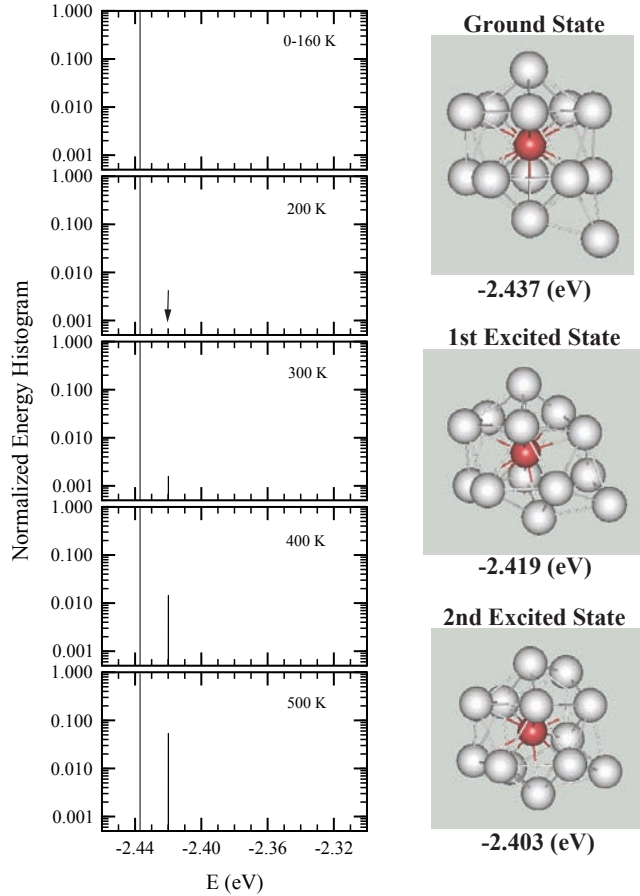


FIG. 4: Same as Fig. 2 but for  $\text{Ag}_{13}\text{Cu}_1$ . Energy histograms were constructed from isothermal Brownian-type MD simulations at temperatures  $T = 0 \sim 160, 200, 300, 400$  and  $500$  K. The arrow at  $T = 200$  K is the first excited state but on the scale of this figure is vanishingly small.

The whole cluster VACF is

$$C(t) = \frac{\sum_{i=1}^n \sum_{j=1}^M \vec{v}_i(t_{0j}) \cdot \vec{v}_i(t_{0j} + t)}{\sum_{i=1}^n \sum_{j=1}^M \vec{v}_i(t_{0j}) \cdot \vec{v}_i(t_{0j})}$$

from which we Fourier-transform to obtain the whole cluster  $\Omega(\omega)$ . In equations above,  $M$  is the total time steps,  $n$  is the total number of atoms,  $\vec{v}_i$  is the velocity of  $i$ th atom in the cluster and

$$E_{total} = \left[ \sum_{i(a)} \frac{p_{i(a)}^2}{2m_a} + \sum_{i(b)} \frac{p_{i(b)}^2}{2m_b} + E_n \right]$$

in which  $i(a)$  ( $i(b)$ ) is  $i$ th atom of type  $a$  (type  $b$ ) and  $E_n$  is the empirical many-body potential defined by Eq. (1).

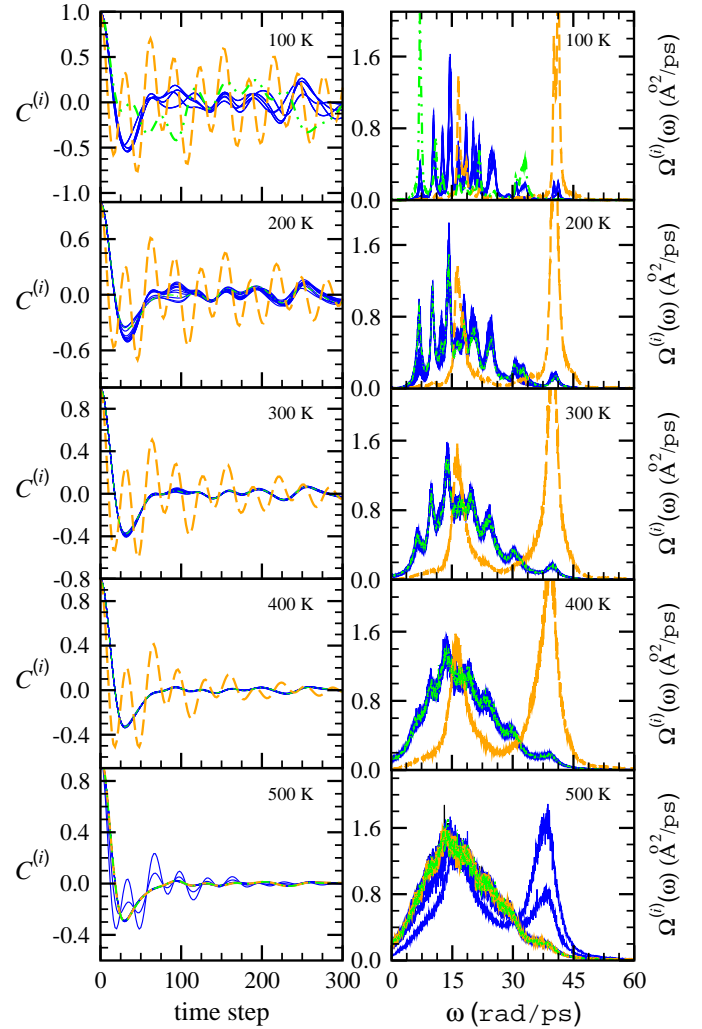


FIG. 5: Temperature variation (100~500 K) of the velocity autocorrelation function (left column) vs. time step (in units of  $5 \times 10^{-15}$  s) and power spectrum vs. frequency  $\omega$  (in units of rad/ps) (right column) for  $\text{Ag}_{14}$  determined from isothermal Brownian-type MD simulation. The particle is colored orange (dashed line) for center atom, green (dash-dot-dotted line) for floating atom and blue (solid line) for the rest of surface atoms. Note that at  $T = 500$  K two atoms, surface or floating, have permuted separately with the center atom (orange—blue).

### III. RESULTS AND DISCUSSION

The ground state structure of both bimetallic clusters have their respective impurity atom resided at the center of the 13-atom icosahedron and their 14th atom "floated" at a site above three triangular shape atoms of which one

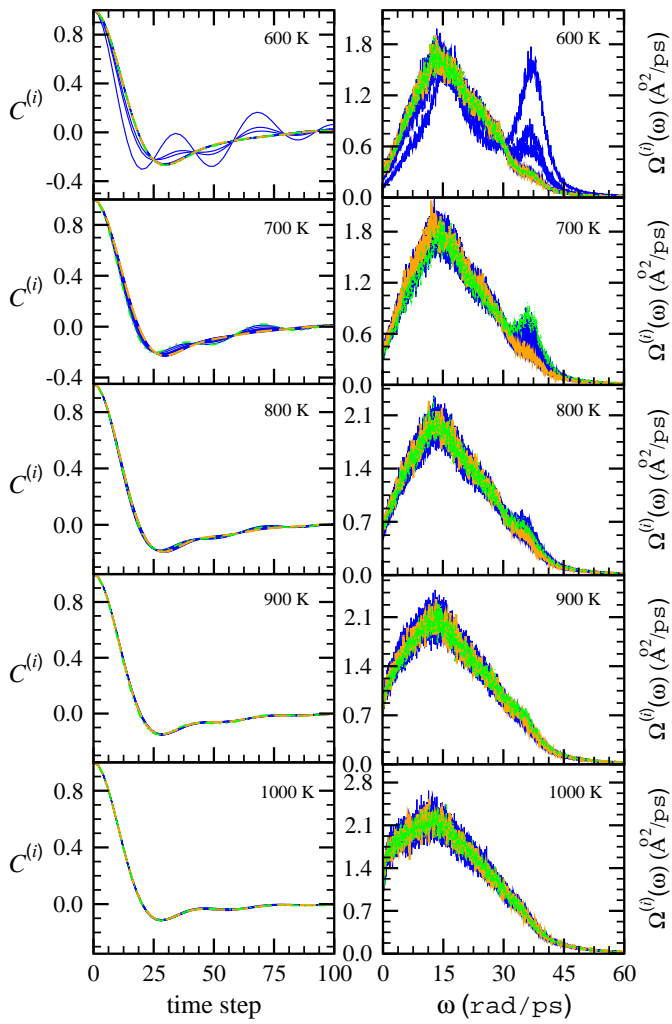


FIG. 6: Temperature variation (600~1000 K) of the velocity autocorrelation function (left column) vs. time step (in units of  $5 \times 10^{-15}$  s) and power spectrum vs. frequency  $\omega$  (in units of rad/ps) (right column) for  $\text{Ag}_{14}$  determined from isothermal Brownian-type MD simulation. The particle is colored orange (dashed line) for center atom, green (dash-dot-dotted line) for floating atom and blue (solid line) for the rest of surface atoms. Note that at  $T = 600$  K three atoms, surface or floating, have separately permuted with the center atom (orange— $\rightarrow$  blue).

is the apex atom and two others pertained to a nearby pentagonal ring. Figure 1 displays the  $C_V$  for the clusters  $\text{Ag}_{14}$ ,  $\text{Ag}_{13}\text{Au}_1$  and  $\text{Ag}_{13}\text{Cu}_1$  and the  $T_{\text{melt}}$  of these clusters which were determined separately from the main maxima of  $C_V$  (indicated by arrows) are approximately 920, 1096 and 1022 K, respectively. It is observed in the same figure that there is a prepeak in the  $C_V$  of  $\text{Ag}_{14}$  but, in contrast, no prepeak is found for both bimetallic clusters. The presence of a  $C_V$  prepeak in  $\text{Ag}_{14}$  can be understood from examining the energy histograms and the cluster structures shown in Figs. 2-4. Generally it can be seen that in the range of temperatures  $T < 500$  K the lowest and first excited states dominate. There are, however, discernible differences. In  $\text{Ag}_{14}$ , the first excited state which describes an atomic structure in which the icosahedron is distorted to permit the adatom residing at a site above four atoms appears first at a lower tempera-

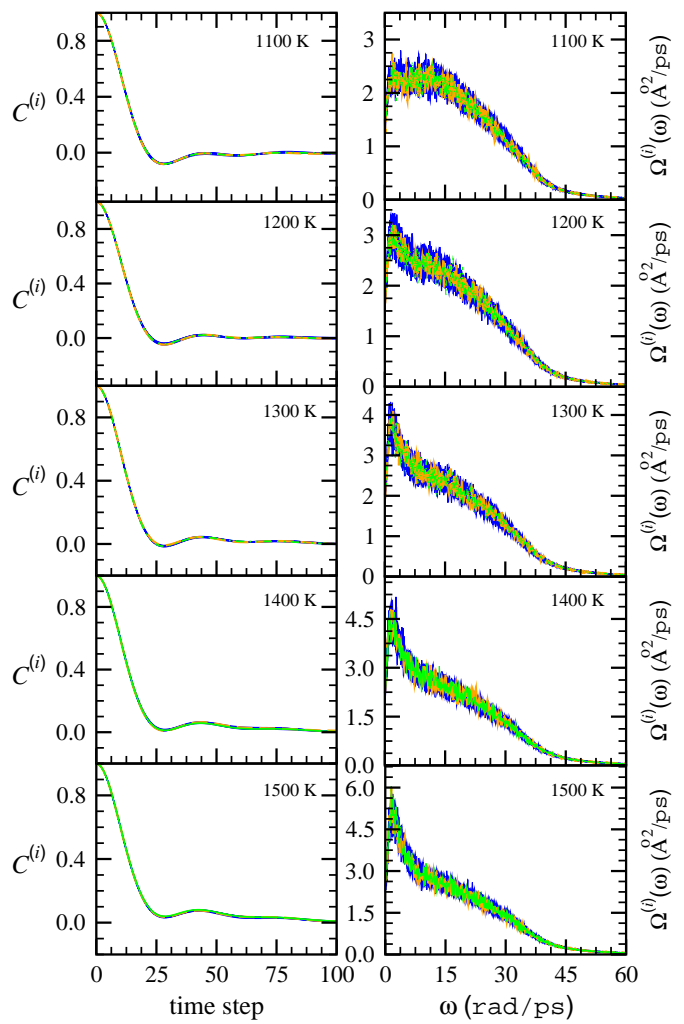


FIG. 7: Temperature variation (1100~1500 K) of the velocity autocorrelation function (left column) vs. time step (in units of  $5 \times 10^{-15}$  s) and power spectrum vs. frequency  $\omega$  (in units of rad/ps) (right column) for  $\text{Ag}_{14}$  determined from isothermal Brownian-type MD simulation. The particle is colored orange (dashed line) for center atom, green (dash-dot-dotted line) for floating atom and blue (solid line) for the rest of surface atoms.

ture  $T = 150$  K. In the temperature range  $150 \leq T < 500$  K the first excited state increases and is accompanied by the second excited state as well. This thermal behavior is in marked contrast to the bimetallic clusters. For the cluster  $\text{Ag}_{13}\text{Au}_1$ , it is in its lowest energy state up to  $T = 140$  K. Its first excited state can be detected at  $T = 200$  K but on the scale of Fig. 3 (indicated by an arrow) is invisible. Then we observe at  $T = 300$  K the first excited state which persists up to  $T < 500$  K. For this cluster, the second excited state appears at  $T = 500$  K. The cluster  $\text{Ag}_{13}\text{Cu}_1$  behaves similarly except that the second excited state is not observed even up to  $T = 500$  K. Accordingly the migrational relocation of the floating atom that leads to the switching of cluster configurations between the ground, first and possibly second excited states (see Figs. 2-4) is relatively easier and at a higher frequency in  $\text{Ag}_{14}$  (recall the discussion above) than the two Ag-based bimetallic clusters. This structural swap among the lowest, first and second excited states which is in fact a dy-

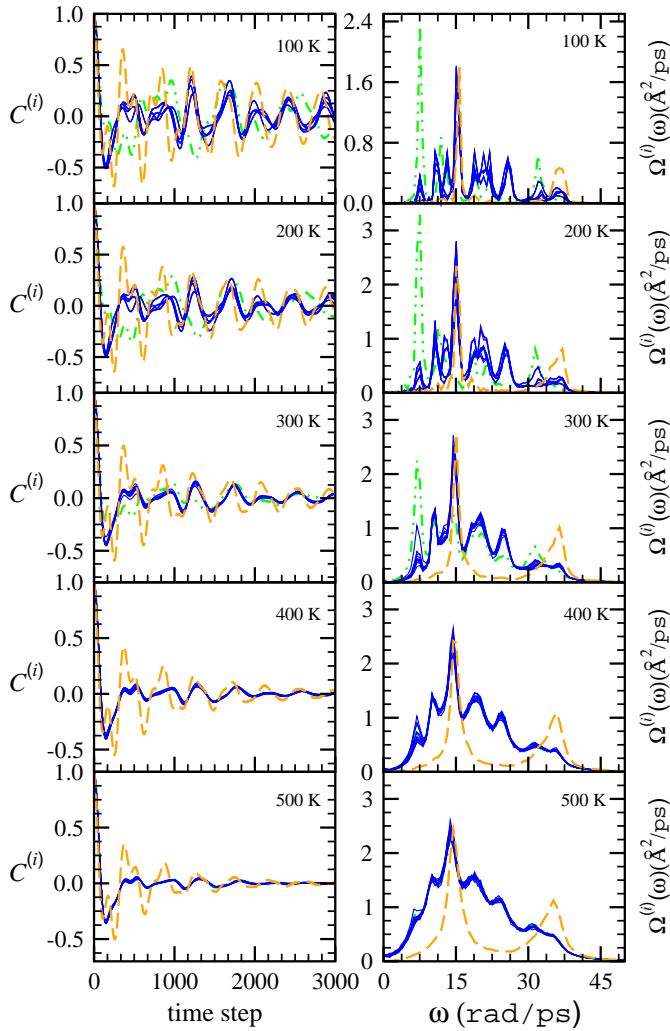


FIG. 8: Temperature variation (100~500 K) of the velocity autocorrelation function (left column) vs. time step (in units of  $10^{-15}$  s) and power spectrum vs. frequency  $\omega$  (in units of rad/ps) (right column) for  $\text{Ag}_{13}\text{Au}_1$  determined from isothermal Brownian-type MD simulation. The particle is colored orange (dashed line) for center atom, green (dash-dot-dotted line) for floating atom and blue (solid line) for the rest of surface atoms.

nodynamical process would result in the conspicuous change of the total energy with temperature and hence the emergence of a prepeak at  $T \simeq 300$  K. We should remark that at higher temperatures the migrational motion is superimposed by permutational isomer transitions involving the surface and floating atoms.

We turn next to the  $C^{(i)}(t)$  and its Fourier-transformed spectral density,  $\Omega^{(i)}(\omega)$ . In Fig. 2, we show the structures of lowest energy and lower excited states of  $\text{Ag}_{14}$ , and in the same figure next to it, we describe the probability of occurrence of these states as a function of temperature by the energy histograms. Our simulated results of  $C^{(i)}$  and  $\Omega^{(i)}$  at different temperatures are displayed in Figs. 5-7. A general characteristic of  $C^{(i)}$  and  $\Omega^{(i)}$  for temperatures  $T < 400$  K is that all of fourteen individual atoms exhibit a typical solid-like behavior; the atoms vibrate at a low frequency value  $\omega_L \simeq 16$  rad/ps and this oscillatory behavior is reminiscent of the infra-red molec-

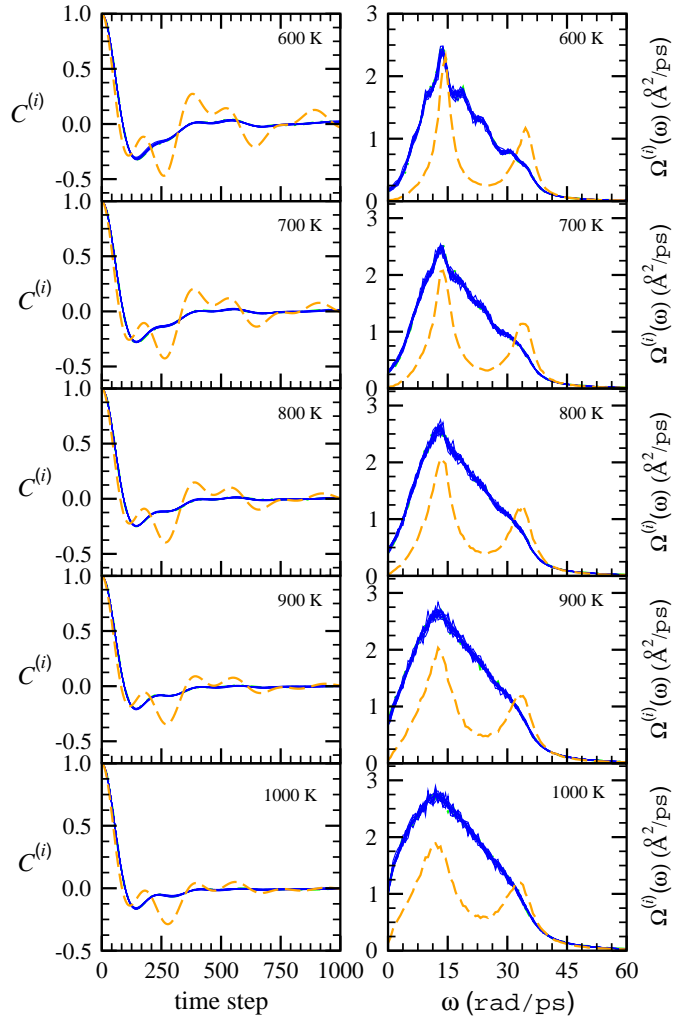


FIG. 9: Temperature variation (600~1000 K) of the velocity autocorrelation function (left column) vs. time step (in units of  $10^{-15}$  s) and power spectrum vs. frequency  $\omega$  (in units of rad/ps) (right column) for  $\text{Ag}_{13}\text{Au}_1$  determined from isothermal Brownian-type MD simulation. The particle is colored orange (dashed line) for center atom, green (dash-dot-dotted line) for floating atom and blue (solid line) for the rest of surface atoms.

ular vibration. The atom at the center of the icosahedron has in addition a high frequency value  $\omega_H \simeq 41$  rad/ps which may be ascribed to the atom being surrounded by an atomic wall. At temperatures  $T = 500 \sim 700$  K one observes permutations between the central atom and a surface atom. Perhaps more interesting is the change in magnitude of the central atom  $\Omega^{(c)}(\omega_H)$  which declines with increasing temperature. This structural change of  $\Omega^{(c)}(\omega_H)$  was observed previously [3] for  $\text{Cu}_{14}$  and  $\text{Cu}_{13}\text{M}_1$  ( $\text{M}=\text{Au}$  and  $\text{Ag}$ ) and has been used to define  $T_{\text{melt}}$ . The definition is based on two criteria. The first criterion is related to the magnitude of the central atom  $\Omega^{(c)}(\omega_H)$ . Since it declines with increasing temperature,  $T_{\text{melt}}$  is the temperature when  $\Omega^{(c)}(\omega_H)$  'dissolves' into the  $\Omega^{(i)}(\omega)$  of the surface ( $i = s$ ) and floating ( $i = f$ ) atoms. The second criterion is associated with the structure of  $\Omega^{(i)}(\omega)$ . At  $T_{\text{melt}}$ , all of fourteen  $\Omega^{(i)}(\omega)$  assume the same structure and share the same low frequency  $\omega_L$ .

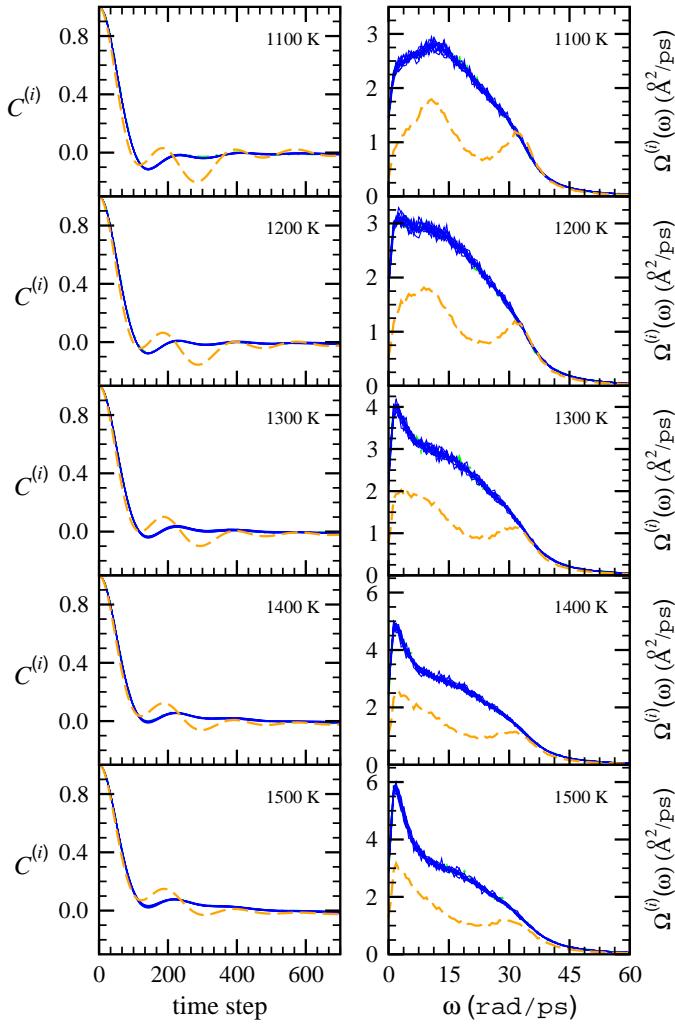


FIG. 10: Temperature variation (1100~1500 K) of the velocity autocorrelation function (left column) vs. time step (in units of  $10^{-15}$  s) and power spectrum vs. frequency  $\omega$  (in units of rad/ps) (right column) for  $\text{Ag}_{13}\text{Au}_1$  determined from isothermal Brownian-type MD simulation. The particle is colored orange (dashed line) for center atom, green (dash-dot-dotted line) for floating atom and blue (solid line) for the rest of surface atoms.

The simultaneous fulfillment of these two criteria yields  $\omega_L \simeq 13$  rad/ps (second criterion) and  $T_{\text{melt}} \simeq 900$  K for  $\text{Ag}_{14}$ . The predicted  $T_{\text{melt}}$  agrees quite well with the  $T_{\text{melt}} \simeq 920$  K indicated by an arrow in Fig. 1.

In Figs. 8-10 and 11-13, we depict  $C^{(i)}$  and  $\Omega^{(i)}$  of  $\text{Ag}_{13}\text{Au}_1$  and  $\text{Ag}_{13}\text{Cu}_1$  respectively. With respect to those of  $\text{Ag}_{14}$  (see Figs. 5-7), we remark the following similarities and differences:

- (a) There exist high frequency modes  $\omega_H$  for the  $\Omega^{(c)}$  of  $\text{Ag}_{13}\text{Au}_1$  and  $\text{Ag}_{13}\text{Cu}_1$ ; the former is located at  $\omega_H \simeq 34$  rad/ps which is lower than the latter  $\omega_H \simeq 39$  rad/ps as well as that of  $\text{Ag}_{14}$  which occurs at  $\omega_H \simeq 38.5$  rad/ps. As in our previous interpretation on Cu-based clusters [3],  $\omega_H$  is translated to come from the central atom being caged by the atomic wall of Ag atoms.
- (b) Applying the two criteria to the  $\Omega^{(i)}$  as we did for  $\text{Ag}_{14}$

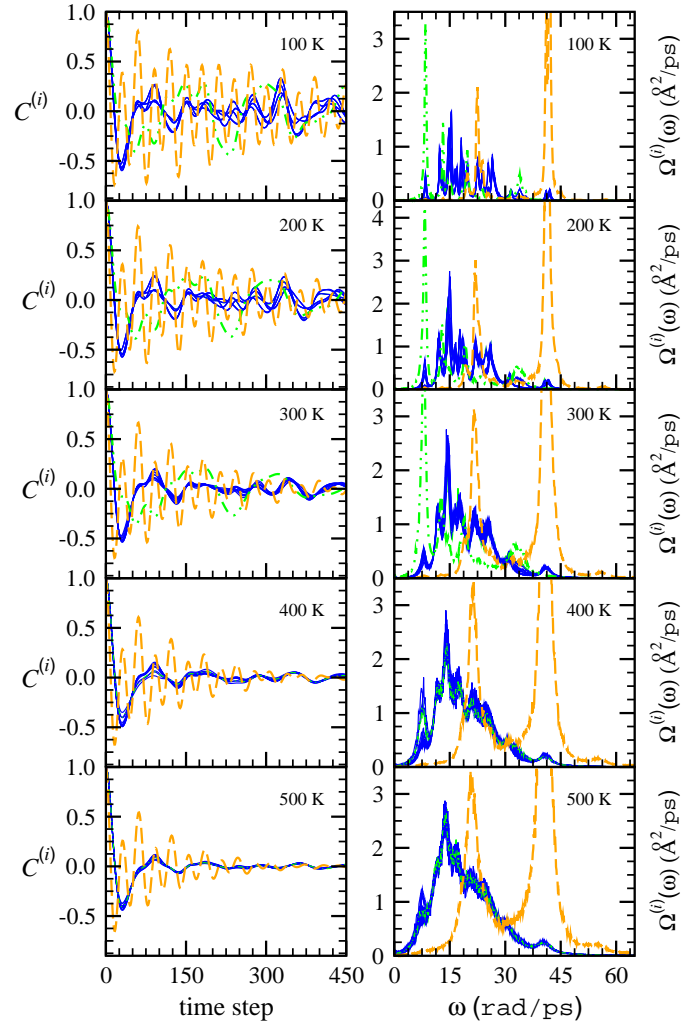


FIG. 11: Temperature variation (100~500 K) of the velocity autocorrelation function (left column) vs. time step (in units of  $5 \times 10^{-15}$  s) and power spectrum vs. frequency  $\omega$  (in units of rad/ps) (right column) for  $\text{Ag}_{13}\text{Cu}_1$  determined from isothermal Brownian-type MD simulation. The particle is colored orange (dashed line) for center atom, green (dash-dot-dotted line) for floating atom and blue (solid line) for the rest of surface atoms.

and also scrutinizing  $\Omega$  (Fig. 14(a)) of  $\text{Ag}_{13}\text{Au}_1$ , we obtain  $T_{\text{melt}} \simeq 1100$  K whose value is pretty close to the  $T_{\text{melt}}$  inferred from  $C_V$ . In arriving at this solid-liquid-like transition temperature we should emphasize that the high frequency mode of  $\Omega^{(c)}$  decreases weakly with increasing temperature from say  $\omega_H \simeq 36$  rad/ps at  $T = 100$  K to approximately 33 rad/ps at  $T = 1000$  K (temperature just before solid-liquid-like transition), although the magnitude of  $\Omega^{(c)}(\omega_H)$  does not vary much and in fact remains low but undiminished. This characteristic feature of  $\Omega^{(c)}$  is similar to that of  $\text{Cu}_{13}\text{Au}_1$  [3] but is quite different from the pure  $\text{Ag}_{14}$  cluster. One plausible cause is that the Au atom has a heavier mass which is about twice that of Ag. Since the small-time limit of VACF is inversely proportional to the mass of the atom [3, 11], the vehement oscillatory frequency  $\omega_H$  of the Au atom within the cage of Ag atoms is relatively smaller and

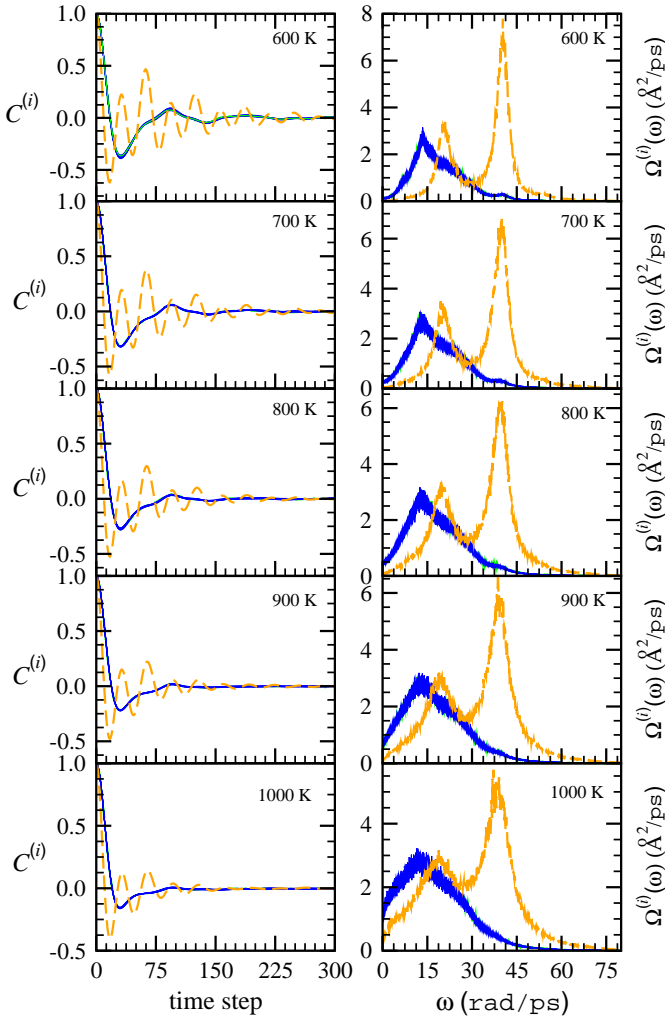


FIG. 12: Temperature variation (600~1000 K) of the velocity autocorrelation function (left column) vs. time step (in units of  $5 \times 10^{-15}$  s) and power spectrum vs. frequency  $\omega$  (in units of rad/ps) (right column) for  $\text{Ag}_{13}\text{Cu}_1$  determined from isothermal Brownian-type MD simulation. The particle is colored orange (dashed line) for center atom, green (dash-dot-dotted line) for floating atom and blue (solid line) for the rest of surface atoms.

it goes on even at high temperatures. This scenario is consistent with the observation that the  $\omega_H$  values of the  $\Omega^{(c)}$  of  $\text{Ag}_{14}$  are relatively higher varying from say  $\omega_H \simeq 41$  rad/ps at  $T = 100$  K to approximately 36 rad/ps at  $T = 800$  K (temperature just before solid-liquid-like transition). The same characteristic feature was previously observed also for  $\text{Cu}_{13}\text{Au}_1$  [3]. There is, however, a slight difference for the latter cluster. Whereas in  $\text{Cu}_{13}\text{Au}_1$  the solid-like behavior is robust even at high temperatures (up to  $T \simeq 1200$  K, signaled by the permutations among central and surface atoms) the solid-like behavior is apparently less severe in  $\text{Ag}_{13}\text{Au}_1$ .

Coming to  $\text{Ag}_{13}\text{Cu}_1$ , here the impurity atom Cu is characterized by a lighter mass (about 1.7 times less than that of Ag). This cluster displays an entirely different picture in  $\Omega^{(c)}$ . The low frequency of  $\Omega^{(c)}$  assumes  $\omega_L \simeq 21$  rad/ps about 7 rad/ps higher com-

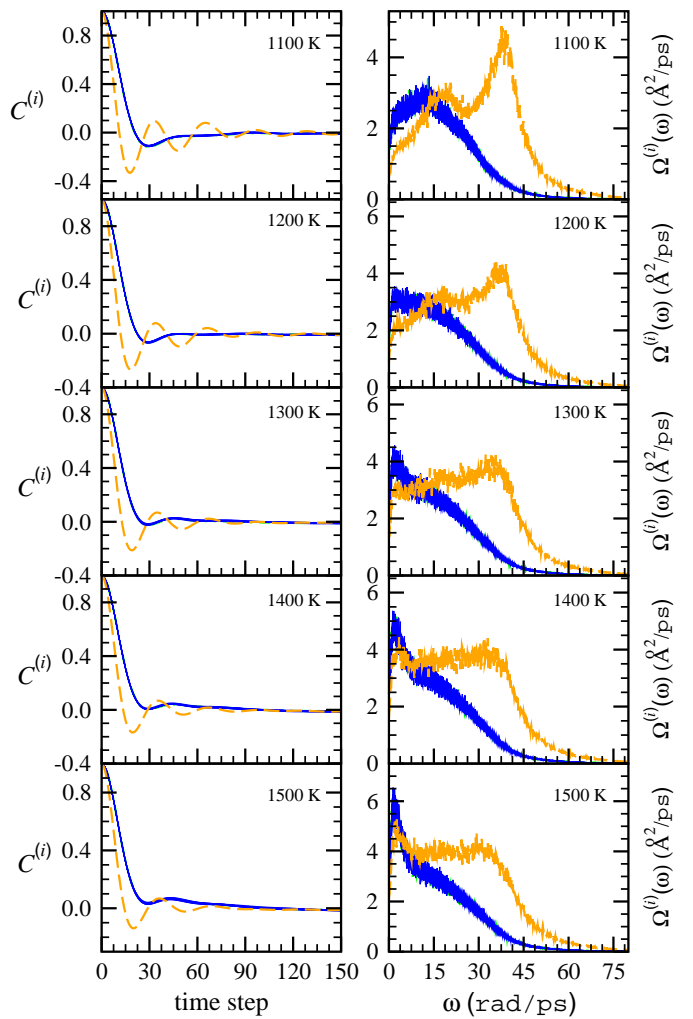


FIG. 13: Temperature variation (1100~1500 K) of the velocity autocorrelation function (left column) vs. time step (in units of  $5 \times 10^{-15}$  s) and power spectrum vs. frequency  $\omega$  (in units of rad/ps) (right column) for  $\text{Ag}_{13}\text{Cu}_1$  determined from isothermal Brownian-type MD simulation. The particle is colored orange (dashed line) for center atom, green (dash-dot-dotted line) for floating atom and blue (solid line) for the rest of surface atoms.

pared with the  $\omega_L$  of the surface  $\Omega^{(s)}$  and floating  $\Omega^{(f)}$ , and its high frequency value is now  $\omega_H \simeq 41$  rad/ps at  $T = 100$  K reducing to approximately 37.5 rad/ps at  $T = 1000$  K (temperature just before solid-liquid-like transition). Notice that the  $\Omega^{(c)}(\omega_H)$  has a distinctly large magnitude. As a result, the first criterion used for stipulating  $T_{\text{melt}}$  fails for this cluster. The reason for this anomalously large  $\Omega^{(c)}(\omega_H)$  may be understood qualitatively by referring to Eq. (1). One can estimate the relative importance of the pair (first term) and many-body (second term) contributions by calculating the ratio  $p_{ij}/q_{ij}$  [12]. As analyzed generally in the work of Doye [12], one would anticipate a progression from potentials that favour icosahedra to decahedra to close-packed and finally disordered structure as  $p_{ij} \longrightarrow 2q_{ij}$  or  $p_{ij}/q_{ij} = 2$ . Now, in replacing a Ag atom by the impurity Cu atom, the ratio  $p_{\text{AgAg}}/q_{\text{AgAg}} = 3.41$  increases to

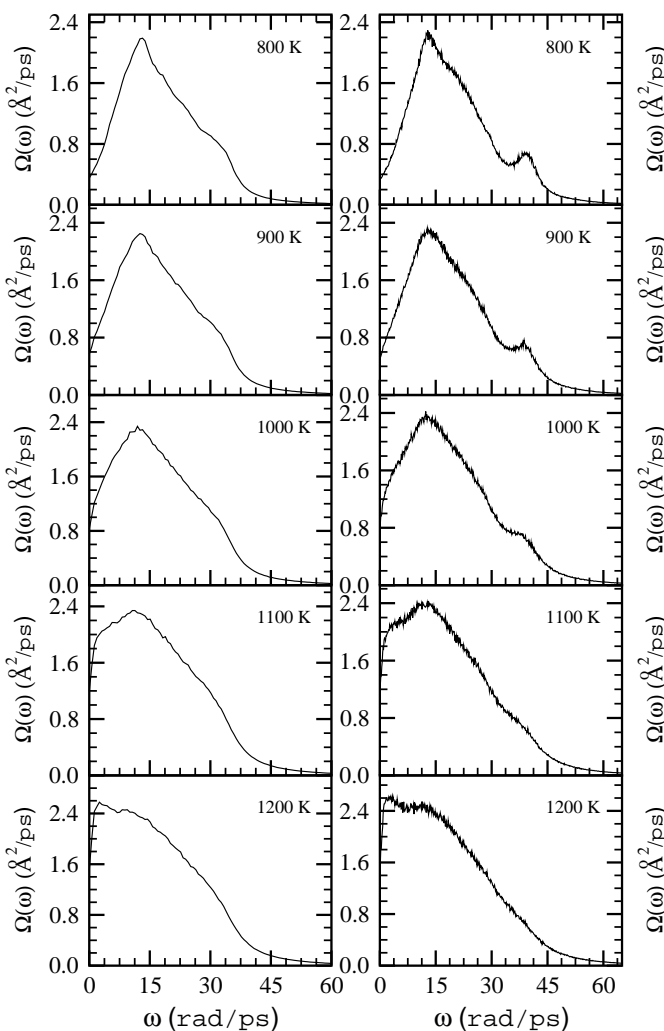


FIG. 14: The whole cluster power spectrum  $\Omega(\omega)$  vs. frequency  $\omega$  for (a)  $\text{Ag}_{13}\text{Au}_1$  (left column) and (b)  $\text{Ag}_{13}\text{Cu}_1$  (right column). The temperature at which the high frequency  $\omega_H$  vanishes (see text) is defined in conjunction with VACF and  $\Omega^{(i)}$  to be the melting temperature.

$p_{\text{Ag}Cu}/q_{\text{Ag}Cu} = 3.81$ . This implies that there is a tendency for this bimetallic cluster to sustain the

icosahedra structure and the central atom Cu whose mass is 1.7 times lighter than Ag atom would have robust contribution coming from the pairwise energy and hence larger  $\Omega^{(c)}(\omega_H)$ . This behavior is in plain contrast to  $\text{Ag}_{13}\text{Au}_1$  whose  $p_{ij}/q_{ij}$  ratio varies from  $p_{\text{Ag}Ag}/q_{\text{Ag}Ag} = 3.41$  to  $p_{\text{Ag}Au}/q_{\text{Ag}Au} = 2.91$ . The many-body embedding energy is apparently more crucial.

To predict the  $T_{\text{melt}}$ , we resort thus to analyzing Fig. 14(b) for the whole cluster  $\Omega(\omega)$  in the range of temperatures  $800 \sim 1200$  K. It is readily seen that the high frequency  $\omega_H$  disappears at  $T \simeq 1100$  K whose value is reasonably close to the  $T_{\text{melt}}=1096$  K determined from the main peak of  $C_V$ .

#### IV. CONCLUSIONS

We have performed isothermal Brownian-type molecular dynamics simulation studies for the specific heat and VACF or its Fourier-transformed spectral density of  $\text{Ag}_{14}$ ,  $\text{Ag}_{13}\text{Au}_1$  and  $\text{Ag}_{13}\text{Cu}_1$ . We observed a prepeak structure in  $\text{Ag}_{14}$  which is absent in the two Ag-based bimetallic clusters. Our analysis showed that the migrational relocation of the floating atom is the cause for such an interesting feature. For the VACF and power spectrum, we found that they can be used as additional variables for portending the melting temperature of clusters. Upon examining the temperature changes of VACF,  $\Omega^{(i)}$  and  $\Omega$  of these three clusters and on the basis of these thermal variations, we predicted their melting temperatures; these predicted values are reasonably close to ones determined at the principal peaks of their respective specific heats. To gain deeper insight into the melting transition, it would be interesting to spur further investigation on such issue as scrutinizing the finite value of  $\Omega^{(i)}(\omega)$  or  $\Omega(\omega)$  at  $\omega = 0$ , a criterion widely used also in the bulk system to signal a transition to liquid state.

#### Acknowledgments

This work is supported (NSC96-2112-M-008-018-MY3) by the National Science Council, Taiwan.

- 
- [1] S. K. Lai, W. D. Lin, K. L. Wu, W. H. Li, and K. C. Lee, J. Chem. Phys. **121**, 1487 (2004).
  - [2] Tsung-Wen Yen, S.K. Lai, N. Jakse, and J.L. Bretonnet, Phys. Rev. B **75**, 165420 (2007).
  - [3] P. J. Hsu, J. S. Lo, S. K. Lai, J. F. Wax, and J. L. Bretonnet, J. Chem. Phys. **129**, 194302 (2008). This reference summarizes some recent studies of clusters which are devoted to using velocity autocorrelation function.
  - [4] J. Jellinek and I. L. Garzon, Z. Phys. D **20**, 239 (1991).
  - [5] Z. B. Güvenc, J. Jellinek, and A.F. Voter, in *Physics and Chemistry of Finite Systems: From Clusters to Crystals*, Vol. 1, edited by P. Jena, S.N. Khanna, and B.K. Rao (Kluwer Academic Publ., Dordrecht, 1992), p.411.
  - [6] M.J. López, P.A. Marcos, and J.A. Alonso, J. Chem. Phys. **104**, 1056 (1996).
  - [7] Young Joo Lee, Jae Yeol Maeng, Eok-Kyun Lee, Bongsoo Kim, Sehun Kim, and Kyu-Kwang Han, J. Computational Chem. **21**, 380 (2000).
  - [8] A. Sebetci and Z. B. Guvenc, Modelling Simul. Mater. Sci. Eng. **12**, 1131 (2004).
  - [9] A. Rapallo, G. Rossi, R. Ferrando, A. Fortunelli, Benjamin C. Curley, Lesley D. Lloyd, G. M. Tarbuck, and R. L. Johnston, J. Chem. Phys. **122**, 194308 (2005).
  - [10] C. Mottet, G. Treglia, and B. Legrand, Phys. Rev. B **46**, 16018 (1992).
  - [11] D.A. McQuarrie, *Statistical Mechanics* (Harper and Row, New York, 1976).
  - [12] J. P. K. Doye, Phys. Rev. B **68**, 195418 (2003); J. P. K. Doye, Computational Mater. Sci. **35**, 227 (2006).